Large-scale distributed watershed modelling for reservoir operations in cold boreal regions

M.E. St. Laurent and C. Valeo

Abstract: The macroscale deterministic hydrologic model, SLURP, was modified and tested on two large watersheds in northern Manitoba, the Taylor River watershed (899 km^2) and the upper Burntwood River watershed (6959 km^2). Calibration and validation of the model on both watersheds between 1985 and 2000 identified a number of model deficiencies and recommendations for improvement. Date-dependent snowmelt rates were replaced with a single constant snowmelt rate, helping to decrease the parameterization of the model. A snowpack temperature deficit model was also incorporated to simulate the effects of snow ripening. These two modifications provided the modelling flexibility needed to control the timing of initial snowmelt and the rate of snowmelt. Annual spring freshet lasts roughly 2 weeks in this region; however, improved model performance was observed well beyond the spring freshet period. These modifications also provided a better representation of the physical processes that delay snowmelt once the air temperature exceeds 0 °C.

Key words: frozen ground, boreal forest, hydrological modelling, snow ripening, snowmelt.

Résumé : Le modèle déterministe hydrologique de grande échelle « SLURP » a été modifié et mis à l'épreuve sur deux grands bassins hydrologiques du nord du Manitoba, celui de la rivière Taylor (899 km^2) et celui de la rivière Upper Burntwood (6959 km^2). L'étalonnage et la validation du modèle sur les deux bassins hydrologiques entre 1985 et 2000 ont permis d'identifier plusieurs faiblesses du modèle et ont suggéré des moyens de l'améliorer. Les taux de fonte des neiges chronosensibles ont été remplacés par un taux unique et constant de fonte des neiges aidant à diminuer le paramétrage du modèle. Un modèle du déficit de température de la neige accumulée a aussi été incorporé pour simuler les effets du mûrissement de la neige. Ces deux modifications ont conféré au modèle la flexibilité requise pour contrôler le moment du début et le taux de la fonte des neiges. La crue nivale annuelle printanière dure environ deux semaines dans cette région. Cependant, le rendement amélioré du système a été remarqué bien au-delà de la période de crue nivale printanière. Ces modifications ont également fourni une meilleure représentation des procédés physiques qui retardent la fonte des neiges une fois que la température dépasse le point de congélation.

Mots-clés : sol gelé, forêt boréale, modélisation hydrogéologique, mûrissement de la neige, fonte des neiges.

[Traduit par la Rédaction]

Introduction

The Province of Manitoba is rich in water resources. Its location captures the drainage of several large river basins, including the Winnipeg, Red, Assiniboine, Saskatchewan, and Churchill rivers. With the construction of the Churchill River Diversion (CRD), nearly all of the flow in these rivers is combined to create the large Nelson River. This renewable resource has allowed for Manitoba Hydro's substantial development of hydroelectric power on the Nelson River. As a resource that is considered "renewable," the Nelson River is continually targeted for further hydroelectric development. Large hydroelectric potential still exists on both the Nelson River and the CRD, and additional development is planned for the near future. Therefore, estimates of water yield are of primary interest to local water resource developers such as Manitoba Hydro. One area of particular interest that requires accurate water yield estimates is the upper and lower Nelson River basins.

The remoteness of the region in conjunction with economic considerations hinder the implementation of additional gauging stations. Estimates of water yield can be used for real-time forecasting of flow inputs for system operations, probable maximum flood derivation for dam safety, modelling of ungauged watersheds, and the establishment of long-term flow records for hydropower planning studies. Not surprisingly, accurate deterministic hydrological modelling of runoff rates and water yield could be used to support these functions.

The high northern boreal forest of the Canadian prairies is a unique ecosystem of coniferous, deciduous, and mixedwood trees amidst mildly rolling terrain with high water tables. The region is of particular interest to several groups,

Received 7 February 2006. Revision accepted 21 September 2006. Published on the NRC Research Press Web site at cjce.nrc.ca on 5 May 2007.

M.E. St. Laurent. Hydro Power Planning Department, Manitoba Hydro, 444 St. Mary Avenue, Winnipeg, MB R3C 3T7, Canada.
C. Valeo.[1] Department of Geomatics Engineering, Schulich School of Engineering, University of Calgary, 2500 University Drive NW, Calgary, AB T2N 1N4, Canada.

Written discussion of this article is welcomed and will be received by the Editor until 31 August 2007.

[1]Corresponding author (e-mail: valeo@geomatics.ucalgary.ca).

 © 2007 NRC Canada

including those involved with the Boreal Ecosystem–Atmosphere Study (BOREAS) (Sellers et al. 1997). The intent of BOREAS is to investigate exchanges of energy, water, heat, CO_2, and trace gases between the boreal forest and the atmosphere in support of the Global Energy and Water Cycle Experiment (GEWEX; Leese 1993) and includes intensive remote sensing and ground data collection in the northern boreal forests of Canada.

The hydrological processes leading to streamflows in the high boreal forest of northern Manitoba are influenced by the subarctic climate, the low-relief terrain, and a diverse array of land features including small lakes, boreal forest cover, muskeg, and swamps. Water storage and its subsequent loss through evapotranspiration are a fundamental component of the basin water balance in northern Manitoba basins (Metcalfe and Buttle 1999). There are unique evapotranspiration processes in the region controlled largely by the variable water table depth and the discontinuous permafrost. The landscape is littered with small wetlands and ephemeral surface depressions in the open-canopy black spruce forest which significantly contribute to evaporation. The macroclimate is characterized by long cold winters followed by short mild summers. During the winter months, snow accumulates to create a temporary storage on the ground surface and within the vegetation canopy. In early winter, water stored in wetlands, lakes, peatlands, and upper soil layers is depleted. Once the excess surficial storage runs off, the streamflow reaches a minimum and is sustained by base flow derived by deeper groundwater storage for the remainder of the winter. The month of May brings rapidly warming temperatures that rise above the melting point of snow, thus releasing large amounts of water over a short period of time. The spring freshet normally creates a very steep rise in the hydrograph that results in the peak annual streamflow. Depending on antecedent conditions, infiltration of meltwater may be impeded by partially frozen ground to create overland flow if soil moisture levels prior to freeze-up were sufficiently high. The formation of this discontinuous permafrost is affected by vegetation, shallow snow cover, and low temperatures, which can lead to deep frost penetration (Anderson and Neuman 1984; Nyberg et al. 2001). As the ground begins to thaw, meltwater enters the soil to replenish the groundwater storage, and river flows recede. Throughout the summer, the groundwater, wetland, and peatland storage, initially recharged by the meltwater, is continuously depleted, causing the streamflow to subside. Many northern river basins contain vast amounts of muskeg–peatland. Muskeg has a hydraulic conductivity that varies substantially with depth, which in turn increases the water retention as the water table drops (Radforth and Brawner 1977). Groundwater is occasionally replenished by large summer rain events that may result in temporary rises in streamflow. As the fall months approach, the groundwater continues to deplete, snowfall begins to accumulate, and water present in the upper soil layer begins to freeze.

The purpose of this paper is to improve the modelling of the hydrological processes in this region for the specific purpose of improving reservoir system operations. Although many studies of forest hydrological processes in northern latitudes (including the NOPEX program in the boreal forest of Sweden (Phersson and Pettersson 1997) and BOREAS conducted in the Boreal Shield ecozone of central Canada) collected vast amounts of hydrological data, the literature shows that there are relatively few basin-scale model applications in northern boreal forests, specifically in northern Manitoba. Published basin-scale modelling specifically for engineering applications includes application of the streamflow synthesis and reservoir regulation (SSARR) model to the lower Nelson River and upper Burntwood River (Crippen Acres Wardrop 1990), but there are a number of limitations to SSARR, including the lack of land cover representation, which presents problems when attempting to apply the model to another watershed without recalibration. The land cover in this region is unique and has unique hydrological processes; hence, some representation of land cover by the model is essential to accurate long-term forecasting. The type of modelling required would involve a model that has enough physical basis that it incorporates land cover type influences on processes, yet at the same time is simple enough conceptually that it does not require a great deal of parameterization. Streamflow prediction for reservoir scheduling can be conducted at a daily time step and does not require sophisticated infiltration routines that are intended to be run at hourly or finer temporal scales, often used in comprehensive hydrological process modelling. The ultimate goal of any model in this particular application is the accurate water yield estimation at a suitable temporal scale.

Thus, a move away from SSARR to the semidistributed land use based runoff processes (SLURP) hydrological model (Kite 1997) was made for a number of reasons. The SLURP model has been calibrated on basins worldwide and of many sizes, ranging from 0.47 km^2 to 1.6 million km^2 (Kite 1978, 1991, 1995; Kite et al. 1994; Haberlandt and Kite 1998; Stolte and Van der Kamp 1999). These basins contain a wide variety of land cover types and terrain, including wetlands, mountainous terrain, prairies, subarctic, and forest. SLURP can be described as an explicit soil moisture accounting (ESMA) model (Beven 2000) because it models relevant catchment processes by a system of connected internal storages with mathematical descriptions of the fluxes between the storages. The main advantage of SLURP is that it has been proven to work well at many scales and geographic locations, and its *conceptual* representation of the watershed provides sufficient physical basis with relatively few parameters that require calibration. SLURP allows the user to choose among a variety of evapotranspiration routines, and the representation of subwatershed units is flexible and simple to parameterize. SLURP also accommodates remotely sensed data such as snow water equivalent, snow-covered area, and cloud cover. The model is also public domain software and includes the source code that can be easily modified for customization.

The literature demonstrates that a wide variety of continuous watershed simulation models like SLURP have been explicitly developed for, or at least applied to, various regions of Canada. A few examples include the semi-distributed hydrologic model using remote sensing (DPHM-RS) applied in Alberta (Biftu and Gan 2001), the distributed vegetation–hydrology model applied in Saskatchewan (Chen et al. 2005), and the WATFLOOD™ model applied in British Columbia, Saskatchewan, Manitoba, and Ontario (Bingeman et

© 2007 NRC Canada

al. 2006). Every model has advantages and disadvantages that may or may not preclude its application to a particular study site for a particular time period. The US Army Corps of Engineers Hydrologic Engineering Center (HEC) series of hydrologic modelling programs, for example, are probably the most widely used and popular models, but the current continuous watershed simulation model in the HEC series was not appropriate for this application because of its black-box nature and because it does not model snowmelt processes well. This work did not evaluate the wide variety of models available to determine which one was the best model for application to these watersheds, but previous experience with SLURP in the study region, the availability of source code, and the theoretical development of the model provided the support required in deciding to use SLURP as opposed to any other model.

Therefore, the objective of this paper is to describe an application of the SLURP hydrological model to northern Manitoba and then demonstrate how the model was improved through only a few simple modifications appropriate for the application in question and the region (northern boreal forest) based on the deficiencies in the initial testing. These modifications can guide others attempting to improve their modelling efforts in regions of similar hydrological response for engineering applications. The paper outlines SLURP model theory and describes the study watersheds used to test the model and how the model was parameterized for this region based on the literature. The initial model applications are provided and discussed, the modifications to the theory based on the deficiencies observed in the initial application are given, and the improved model application is presented and discussed.

SLURP hydrological model

The SLURP model divides a basin into hydrologically consistent subareas called aggregation simulation areas (ASA), similar to a subwatershed. Each ASA is further subdivided into a number of subareas, each representing a unique type of land cover.

The SLURP model employs a simple vertical water balance (Fig. 1) at a daily time step on every land cover within each ASA. The model consists of four storages or tanks, namely the canopy storage, snow storage, rapid storage, and slow storage. The first tank involves additions through canopy interception and losses through evaporation. Interception of precipitation by the tree canopy is modelled empirically using

$$[1] \qquad I = \mathrm{LAI} \times AP^B$$

where I is the interception per unit LAI, P is the precipitation, A and B are interception coefficients, and LAI is the leaf area index. Intercepted precipitation is added to the canopy storage (with capacity CC) until it reaches a maximum capacity $\mathrm{CC_{max}}$. The canopy capacity is related to LAI as follows:

$$[2] \qquad \mathrm{CC_{max}} = \mathrm{LAI} \times \mathrm{CC}$$

Evapotranspiration (ET) is calculated using the Spittlehouse–Black method. Soil water limited ET rate (E_{swl})

Fig. 1. The SLURP water balance method. ET, evapotranspiration.

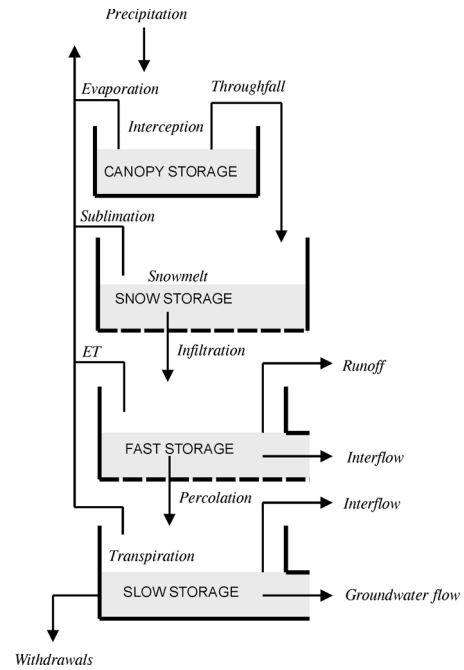

and energy-limited ET rate for water (E_{ew}) and for soil surfaces (E_{es}) are determined using

$$[3] \qquad E_{\mathrm{ew}} = \alpha_{\mathrm{w}}[s/(s+\gamma)](R_{\mathrm{n}} - G)$$

$$[4] \qquad E_{\mathrm{es}} = \alpha_{\mathrm{s}}[\mathrm{s}/(s+\gamma)](R_{\mathrm{n}} - G)$$

and

$$[5] \qquad E_{\mathrm{swl}} = \beta[\mathrm{SS} - (\mathrm{SS_{max}} \times \mathrm{wp})/\mathrm{SS_{max}}(\mathrm{fc} - \mathrm{wp})]$$

where α_{w} is the Priestly–Taylor coefficient from water, s is the slope of the saturation vapor pressure curve, γ is the psychometric constant, R_{n} is the daily net radiation flux density, G is the daily soil heat flux density, α_{s} is the Priestly–Taylor coefficient from soil, β is an empirical constant, SS is the current soil water content, $\mathrm{SS_{max}}$ is the possible soil water content, fc is the field capacity, and wp is the wilting point.

The second tank describes snow accumulation and snowmelt. If the daily mean temperature is below or equal to the critical temperature, the precipitation is considered to be snowfall and accumulates in snow storage. If the mean temperature is above a critical temperature, then the snowpack is depleted using the degree-day method and the snowmelt (S_{m} in mm) enters the fast storage tank. The degree-day method is given as

$$[6] \qquad S_{\mathrm{m}} = S_{\mathrm{p}}R(T - T_{\mathrm{c}})$$

where R is the snowmelt rate (mm/(d·°C^{-1})), T is the daily mean temperature (°C), T_{c} is the critical temperature (°C), and S_{p} is the depth of the snowpack (mm). Two snowmelt rates R are used, one for July (R_{Jul}) and one for January (R_{Jan}), and daily melt rates are interpolated (parabolically) between these two values.

The fast storage tank is a linear reservoir with a maximum capacity $S_{\mathrm{f}}^{\mathrm{max}}$ (mm) and a dimensionless retention constant k_{f} such that

© 2007 NRC Canada

$$S_f = k_f Q_f \quad [7]$$

where Q_f (mm) is the fast storage flow in the time step, and S_f is the moisture stored in fast storage. The fast storage tank will contain an initial moisture content and can receive snowmelt water and throughfall that is over and above canopy storage. If the water supply from rainfall or snowmelt is greater than the given infiltration rate, or if water in the fast tank has reached the maximum capacity, then the water is depleted to surface runoff. The infiltration rate is related to the amount of water in the fast storage tank, the fast tank capacity, and some specified maximum possible infiltration rate I_f^{max} (mm). The last tank, or slow storage tank, models the process of groundwater flow. Like fast storage, groundwater flow Q_b (mm) is calculated based on the linear reservoir concept with a maximum capacity S_s^{max} (mm) and a retention constant k_s (d).

Runoff from each land cover is routed to the nearest stream using the velocity form of Manning's equation in conjunction with average slopes and average overland flow distances for each land cover within the ASA. Channel routing between ASAs is conducted in this study using the Muskingum method.

Study area

The Taylor River watershed (899 km^2) and the upper Burntwood River watershed (6959 km^2) are located in the Nelson River basin in the high boreal forest of northern Manitoba (Fig. 2). These watersheds were selected because of Manitoba Hydro's continued interests in developing water resources in this area and the lengthy historical record of streamflow gauging available for these two watersheds of differing sizes. The Taylor River watershed is comprised of gray luvisolic soils on clay; the headwaters of the upper Burntwood River are in dystric brunisolic sandy soils, the middle reaches are in hard rock outcrops, and the lower reaches are in wooded organic mesisols and are made up mainly of flat bogs (Agriculture Canada 1986). The predominant tree species throughout the Nelson River basin is black spruce. The forest is characterized by homogeneous stands of black spruce, jack pine, white birch, and trembling aspen (McKnight 1993). The dominant type of land cover in northern Manitoba is muskeg. Muskeg is often referred to as bogland, organic terrain, or peatland. The Nelson River basin has low topographic relief, with elevations ranging from 239 to 367 m in the upper Burntwood River basin and from 187 to 281 m in the Taylor River basin. The terrain can be described as hummocky, with bogs and fens occurring in low-lying areas (Metcalfe and Buttle 1999). Average total annual precipitation is 535.6 mm, with 33% occurring as snow. The average snow water equivalent is approximately 200 mm annually. The coolest month of the year, January, experiences an average daily maximum temperature of –19.5 °C and an average daily minimum of –0.6 °C. The warmest month of the year, July, experiences an average daily maximum temperature of 22.6 °C and an average daily minimum of 8.8 °C.

A 100 m resolution digital elevation model (DEM) was created for the study area using a geographic information system (GIS). High-resolution land cover data were obtained from the Forest Resource Inventory of Manitoba and reclassified into the following seven land cover classes: coniferous trees, deciduous trees, mixed trees, muskeg, impervious, water, and marsh. Physiographic parameters such as ASA area, distance, and elevation were computed using a GIS for a total of seven ASAs for the Taylor River watershed and 11 ASAs for the upper Burntwood River watershed. These ASAs are shown in Fig. 3. Sixteen years of meteorological and hydrometric data obtained from Environment Canada for the period 1985–2000 were used for model calibration and validation. These data were representative of a wide range of meteorological conditions with several wet, dry, and median years. Hydrometric data were only available for gauges situated at the basin outlets, and Fig. 2*b* shows the locations of the meteorological stations.

SLURP model parameters were selected from the vast amount of literature generated by the BOREAS projects (Sellers et al. 1997) and the NOPEX program (Phersson and Pettersson 1997). The processes and the parameter selection are detailed in the next three sections.

Fig. 2. Location of the upper Burntwood River and Taylor River basins.

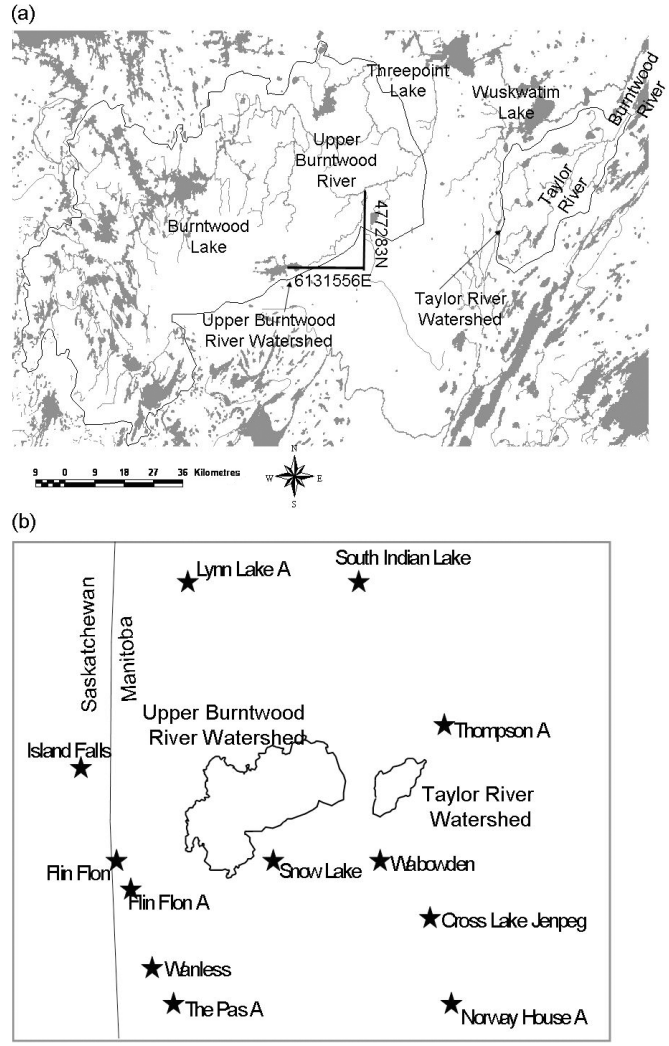

© 2007 NRC Canada

Fig. 3. Aggregation simulation areas (ASAs) for the upper Burntwood River watershed (1–11) and the Taylor River watershed (1–7).

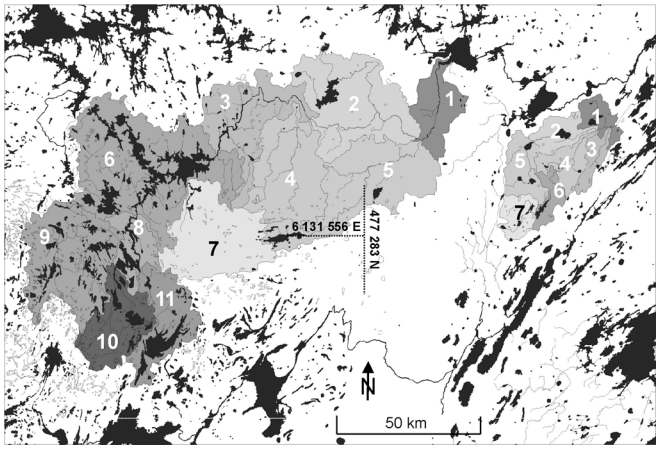

Watershed parameters related to interception and evapotranspiration

The SLURP model requires monthly LAI values for each land cover. The LAI are often derived from normalized difference vegetation indices (NDVI) and estimates of the maximum value of LAI using the linear relationship of Yin and Williams (1997). Monthly NDVI values were obtained from the US Geological Survey. The maximum LAI values for the various types of land cover modelled in this study were obtained from the literature, including Kite and Spence (1994), Newcomer et al. (2000), Kite (2002), and Nickeson et al. (2002). Other values not found in the literature were assumed based on similarities to other land cover types.

Price et al. (1997) found that the significant moss layer present in the boreal forest greatly contributed to the interception of precipitation, a contribution that was nearly as great as that from forest interception. Price et al. found a definitive moss interception capacity in the range of 15–47 mm. Other studies (Grelle et al. 1997; Kite 1998) found the coniferous canopy capacities to be less than the 15–47 mm range. A conservative moss capacity of 15 mm is chosen for the forest covers and 0 mm for the impervious and marsh covers. Price et al. also found that the evaporation from the forest floor made up a very large component (roughly 25%) of the total evaporation in the BOREAS NSA. Thus, the composite canopy capacity will comprise both the coniferous canopy and moss capacities for this study. This results in a composite canopy capacity of 30 mm for the coniferous treed cover at maximum LAI. To account for the effects of the moss layer on evapotranspiration and interception, the maximum value LAI that is used to scale the LAI was increased by 25% for the coniferous, mixed, deciduous, and muskeg land covers. Table 1 lists the estimates of these parameters.

The Spittlehouse method of estimating ET incorporates a soil water limitation to ET, thus providing a better physical representation of ET processes. This is important in the muskeg-dominated environment of the boreal forest where ET is sharply reduced once the soil moisture falls below a certain level (Goode et al. 1977; Phersson and Pettersson 1997; Buttle et al. 2000). Spittlehouse (1989) reported α_s values of 1.26 for crop–grassland and 0.80 for British Columbia coniferous forest. Values of β ranged from 10 mm/d for Douglas-fir to 34 mm/d for pasture. If there are no data, Spittlehouse recommends estimating β using the assumption that soil moisture begins to limit ET once the soil store fraction is 0.30 and ET/α_s = 4.0 mm/d. This assumption may be expressed as β/α_s = 13 mm/d. This results in values of β = 10 mm/d when α_s = 0.80, and β = 16 mm/d when α_s = 1.26. For this study, the first set of values is used for the forest covers, and the second set of values is used for the impervious and marsh covers.

Soil properties

Estimates of field capacity and wilting point are based on a typical soil. The soil profile for this study area as generalized by Metcalfe and Buttle (2001) consists of a peat layer over a silty clay layer. The *Hydrology handbook* (ASCE 1996) specifies an average field capacity of 0.36 and wilting point of 0.21 for silty clay soils. The US Department of Agriculture specifies a field capacity of 0.42 and a wilting point of 0.26 for the same soils (Saxton 2002). This study then assumes a field capacity of 0.39 and a wilting point of 0.23 for all land covers, which are rough averages of the two other values.

Permafrost is discontinuous throughout the area (Peddle and Franklin 1993); according to Brown (1977), muskeg and permafrost are very closely related, as peat influences the formation of permafrost. The peat thickness varies considerably throughout the boreal forest, however, the thickness of the active layer is fairly uniform at 1–2 ft (1 ft = 0.3048 m) in depth (Brown 1977). The capacities of the fast and slow storage tanks can be estimated based on field data. Metcalfe and Buttle (2001) measured the organic layer thickness, mean porosity of the organic layer (0.813), and mean porosity of the silty clay layer (0.314) at various locations during the BOREAS studies. In this study, the upper 1 m of soil is assumed to represent the fast storage tank. The initial estimate for the slow storage tank will equal that of the fast storage tank. The mean porosities for the organic and silty clay layers were applied to the estimated soil thickness for each cover and were used to estimate the storage capacities as shown in Table 1. The model default values are used as initial retention constants for the fast and slow storage tanks, k_f and k_s, respectively. The slow storage content is initialized by preceding all model runs with an additional year of simulation time.

In the forested areas of the BOREAS NSA, Metcalfe and Buttle (2001) found the saturated hydraulic conductivity to range from 2.0×10^{-3} m/s at the surface to 2.0×10^{-7} m/s at the silty clay interface. In flooded areas, they found that the saturated hydraulic conductivity was too rapid to measure and near zero at the silty clay interface. This translates to a nearly limitless infiltration rate into the organic layers in both the forested and wetland environments. In general, the maximum saturated infiltration rate, I_f^{max}, will be maintained at a relatively high value so as not to create overland runoff under normal conditions. A value of 100 mm/d is used for all types of land covers.

Snow processes

Metcalfe and Buttle (2001) provided sufficient information to allow for the calculation of the snowmelt rates during

© 2007 NRC Canada

Table 1. Values of the model parameters for each land cover type in the Taylor River and upper Burntwood River watersheds.

Parameter	Land cover type						
	Coniferous	Deciduous	Mixed	Muskeg	Impervious	Water	Marsh
Land cover (%)*							
Taylor River	34.28	2.82	6.02	37.84	7.34	5.12	6.55
Upper Burntwood River	45.15	2.86	6.97	25.74	5.88	8.73	4.67
Maximum leaf area index (LAI)*	5.38	10.00	9.75	4.38	2.00	0	2.00
Canopy capacity (mm)*	5.58	4.29	4.33	6.22	2.79	0	2.79
Interception coefficients							
A	1.0	1.0	1.0	1.0	0.5	0	1.0
B	1.0	1.0	1.0	1.0	1.0	1.0	1.0
Priestly–Taylor α_w							
Taylor River	1.36	1.36	1.36	1.36	2.14	2.14	2.14
Upper Burntwood River	1.76	1.76	1.76	1.76	2.77	2.77	2.77
Priestly–Taylor α_s							
Taylor River	2.14	2.14	2.14	2.14	2.14	2.14	2.14
Upper Burntwood	2.77	2.77	2.77	2.77	2.77	2.77	2.77
β (mm/d)							
Taylor River	17.0	17.0	17.0	17.0	27.2	27.2	27.2
Upper Burntwood River	22.0	22.0	22.0	22.0	35.2	35.2	35.2
Soil field capacity (fraction)*	0.39	0.39	0.39	0.39	0.39	—	0.39
Soil wilting point (fraction)*	0.23	0.23	0.23	0.23	0.23	—	0.23
Fast storage capacity, S_f^{max} (mm)	407.8	407.8	407.8	492.9	365.0	0	100.0
Fast storage retention constant, k_f	32.7	32.7	32.7	13.2	18.9	1.0	5.0
Slow storage capacity, S_s^{max} (mm)	58.4	58.4	58.4	27.6	375.0	1000.0	500.0
Slow storage retention constant, k_s	517.3	517.3	517.3	393.2	262.5	3.0	50.0
Max. infiltration rate, I_f^{max} (mm/d)*	100	100	100	100	100	—	100
Snowmelt rate (mm/(d·°C^{-1}))							
January, R_{Jan}	0	0	0	0	0	0	0
June, R_{Jul}	0.5	0.5	0.5	0.5	0.5	0.5	0.5
Albedo*							
Surface	0.130	0.160	0.145	0.140	0.152	—	0.152
Max. snow	0.500	0.500	0.500	0.500	0.780	0.780	0.780
Min. snow	0.370	0.370	0.370	0.370	0.370	0.370	0.370

Note: Parameters marked with an asterisk were estimated from the literature, and all others were calibrated during the calibration process.

the 1994 snowmelt period at the BOREAS NSA. They provided the average melt rates, the melt period (11 April – 5 May), and the number of melt days (14 d). The melt rates (mm/(d·°C^{-1})) were back-calculated by dividing the average melt rate (mm/d) during the melt period by the average number of degree-days during the melt period (°C) using the daily average temperatures recorded by BOREAS at the NSA. The values obtained and as shown in Table 1 are used as initial estimates for this study and represent both January and July snowmelt rates. As this parameter is very sensitive and largely controls the timing of the spring freshet, however, it is calibrated.

SLURP model calibration and validation

Calibration

The calibration process involved manually adjusting a number of parameters to improve model performance. These parameters included the retention constant of the slow storage tank (k_s), the maximum capacity of the slow storage tank (S_s^{max}), the maximum capacity of the fast storage tank (S_f^{max}), the retention constant of the fast storage tank (k_f), the January and July snowmelt rates (R_{Jan} and R_{Jul}), the initial contents of the slow and snow storage tanks, both Muskingum routing parameters, and an interception coefficient *A*. The Nash and Sutcliffe efficiency (NSE) (Nash and Sutcliffe 1970) and the deviation of runoff volumes (DV) are used as statistical measures of the goodness of fit of the SLURP model results for this study. Calibration was conducted both manually and using the SCE-UA automatic calibration routine built into the SLURP model, version 11.2. A few of the SLURP storage tanks required initial estimates at the start of the simulation. The initial contents of the slow storage tank were manually adjusted until the initial simulated flow matched the initial observed flow. Initial contents of the fast storage tank cannot be specified within SLURP. The start date for the model simulation was chosen to be September 1 so that the initial contents of the snow storage tank could be set to zero.

Initial application of SLURP to the Taylor River watershed in 1996 demonstrated that base flow dominates the hydrograph but is significantly overestimated by the model. The year 1996 was chosen because it was a median year

© 2007 NRC Canada

from a meteorological perspective. Calibration for this year resulted in an NSE of 74.5% and a DV of 21.8%. Of the 25.5% deficiency in NSE, the majority is directly attributable to the simulation during the snowmelt runoff period (17 May – 30 June) and the minority is due to modelling error during the fall period (9 September – 31 October). The simulated spring peak is found to be 22.1% lower than the observed spring peak. The simulated time of peak for the spring freshet occurs 9 d later than the observed time to peak. The peak flows during the fall months are greatly overestimated by SLURP, with the simulated fall peak resulting in a discharge 1084.6% greater than the observed discharge. The time of peak occurs 14 d earlier than the observed time of peak during the fall months. Tables 1 and 2 show the final calibrated parameters for the Taylor River calibration in 1996.

The annual DV indicated that the annual runoff volume for the majority of the validation years was overestimated for the Taylor River during both the spring and summer periods. This indicates that the SLURP model is not removing the required volume of water from the system through the process of ET. Hence, the ET parameters were increased manually until the DV for all test years was in best agreement with the observed DV. Thus, the calibration took part in two parts: (*i*) with the exception of the parameters governing ET, the calibration parameters were only adjusted using model output during 1996; and then (*ii*) the ET parameters were adjusted so as to obtain the best fit using the entire 16 year period. Table 3 shows modelling efficiencies for the calibration to the Taylor River simulations.

Table 2. Final Muskingum routing coefficients for the Taylor River and upper Burntwood River watersheds.

Watershed	Aggregation simulation area (ASA)	*X*	*K* (d)
Taylor River	1	0.0012	0.7070
Upper Burntwood River	1	0.1200	1.5000
Taylor River	2	0.0000	0.7856
Upper Burntwood River	2	0.1600	1.9500
Upper Burntwood River	3	0.1100	2.1200
Taylor River	4	0.5000	0.1663
Taylor River	6	0.2418	0.7070
Upper Burntwood River	6	0.1400	3.7700
Upper Burntwood River	8	0.1300	0.5700

Note: *K*, travel time of flood wave in a river reach; *X*, weighting factor.

Table 3. Modelling efficiencies for SLURP calibration to the Taylor River and upper Burntwood River watersheds.

	Taylor River		Upper Burntwood River	
Year	NSE (%)	DV (%)	NSE (%)	DV (%)
1985	71	–22	44	–35
1986	76	–16	33	–44
1987	79	3	56	1
1988	—	—	16	57
1989	—	—	–193	61
1990	—	—	69	29
1991	—	—	77	29
1992	75	18	75	–15
1993	27	–10	76	5
1994	28	1	11	–5
1995	58	31	85	3
1996	72	–6	74	9
1997	89	–6	68	–8
1998	42	–16	26	–29
1999	—	—	40	11
2000	55	–8	44	–1
Avg.	61	±12	37	±21
Max.	89	31	85	61
Min.	27	–22	–193	1

Note: NSE, Nash and Sutcliffe efficiency; DV, deviation of runoff volumes.

Validation and recalibration

The simulated hydrographs for all validation years for Taylor River show some response to snowmelt well in advance of the observed hydrographs. Figure 4 shows the simulated and observed hydrographs for 1997 and the temperatures and precipitation intensities in that period. The delay in the observed streamflow response snowmelt is characteristic of a ripening snowpack. In SLURP, the degree-day snowmelt algorithm generates snowmelt and routes it to the fast storage tank on any day when the air temperature exceeds 0 °C, resulting in the hydrograph's sudden response to snowmelt. In nearly all validation years the simulated spring hydrograph peak coincided with the final snowpack depletion. It is likely that the simulated snowpack is not depleting as quickly as it is in nature. This problem is inherent due to the date-dependent snowmelt rates that SLURP uses. The snowmelt rates were lowered to alleviate the onset of snowmelt runoff. It is apparent, however, that this has the adverse effect of prolonging the snowmelt runoff period. The recession rate during the spring freshet and during large summer and fall rain events matches very well in nearly all validation years. This indicates that interflow and percolation are being modelled with reasonable accuracy. The August to December period of 1997 was a very wet period with some very large rain events. The simulation fits extremely well over this period, with NSE of 90% and DV of –6%. The time to peak and the peak flow magnitudes match well. The steep discharge peaks and extended recession limbs are well simulated, particularly during the 14 October – 31 December period when the fast storage tank depletes and the discharge approaches base flow conditions.

The same calibration parameter set used for the Taylor River watershed was applied to the upper Burntwood River watershed and was found to overestimate the volume of runoff for 13 of the 16 validation years for the upper Burntwood River, indicating insufficient ET. Significant evaporation occurs from Burntwood Lake and the many other lakes located in the headwaters of this basin. Many of these lakes receive a continuous supply of water from the upstream headwaters of the basin. Hence, evaporation from these lakes is generally not limited by water availability and is likely to be near the potential evaporation. The model ET component combines both evaporation and transpiration into a single set of ET parameters, and thus only these parameters (α_w, α_s, and

© 2007 NRC Canada

Fig. 4. Simulated and observed hydrographs for Taylor River for 1997. Dates are given as day/month/year.

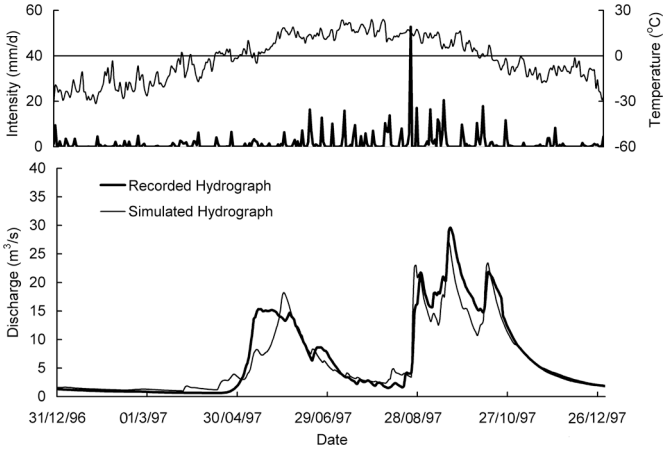

Fig. 5. Simulated and observed hydrographs for upper Burntwood River for 1995. Dates are given as day/month/year.

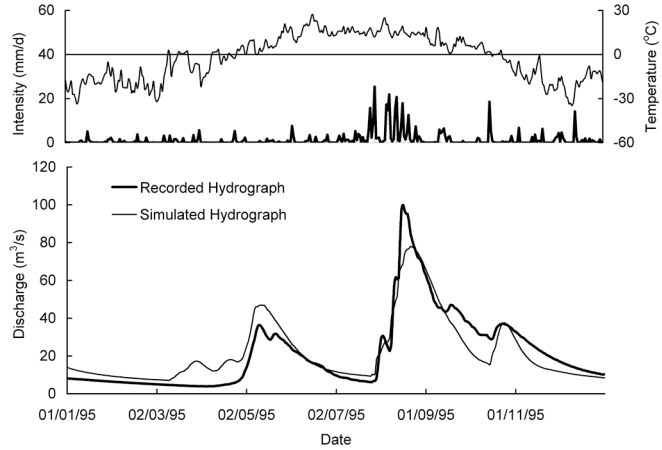

β) were adjusted (to accommodate the elevated evaporation rates) for the upper Burntwood River watershed and are shown in Table 1 with the parameter set used on both watersheds. The large lakes in the watershed also attenuate the hydrographs. A single set of stage–discharge and stage–volume curves was developed to dampen the peak flows and recession rates that are present in the simulations. The volume curve, discharge curve, and Muskingum routing coefficients were manually adjusted until the simulated hydrographs displayed a reasonable fit to the observed hydrographs. The efficiencies for the calibration to the upper Burntwood River watershed involve adjustments to the ET parameters and the Muskingum routing parameters (shown in Tables 1 and 2), but all else remains the same. These efficiencies are shown in Table 3. Figure 5 shows the simulated and observed hydrographs for 1995. The modelling deficiencies observed in the upper Burntwood River watershed simulated hydrographs are similar to those observed in the Taylor River simulated hydrographs and include the following: (*i*) the volume of runoff and peak flows are underestimated during the spring freshet, (*ii*) flows in the late summer are overestimated, (*iii*) the generation of snowmelt runoff is premature, and (*iv*) the timing of the spring freshet peak is delayed in the majority of the test years.

SLURP modifications

Frozen soil and infiltration properties

Permafrost is discontinuous throughout the Nelson River basin (Peddle and Franklin 1993). Elsewhere, the ground is seasonally frozen, thawing completely at some point after the snowmelt period. Metcalfe and Buttle (1999) measured active layer depth during the 1995 snowmelt period at the BOREAS Northern Study Area (NSA), located in close proximity to the Taylor River. They found mean thaw depth to be greatest in the forested landscape and least in wetlands and open forested areas. They observed that ice lenses in larger wetlands quickly became discontinuous during spring snowmelt and thawed completely by the end of the snowmelt period. They also found that the uplands were carpeted by a dry insulating moss layer that maintained permafrost at depth. Metcalfe and Buttle (2001) also observed that frost depth was thicker at wetland margins due to the presence of a thinner insulating peat layer.

According to Brown (1977), muskeg and permafrost are very closely related. During the summer, the surface layers of peat become relatively dry through evaporation. The thermal conductivity of the peat is low, and hence warming of the underlying soil is impeded. The lower peat layers gradually thaw downward and become wet as the ice layers in the seasonally frozen layer melt. In autumn, surface soil moisture increases due to reduced ET rates. When peat freezes, its thermal conductivity increases considerably. Permafrost results when the right conditions under the peat exist such that the temperature remains below freezing throughout the year.

Many field studies have shown that frozen soils decrease or increase infiltration rates depending on antecedent moisture conditions (Zhao and Gray 1997, 1999; Buttle et al. 2000). Simulation results showed that during the spring snowmelt period a small storage capacity and (or) diminished infiltration capacity are required to limit infiltration and generate increased runoff. During the summer months, a much larger soil storage capacity is required to absorb all but the largest rain events. Hence, this modelling deficiency impacts both the snowmelt period of the hydrograph and the summer period of the hydrograph. Zhao and Gray (1999) present a simple correlation function for estimating snowmelt infiltration into frozen soils developed using the results from a numerical model called heat and water transport in frozen soils (HAWTS). The HAWTS model was run for various soil conditions in both a prairie and a boreal forest setting. Zhao and Gray show that infiltration into frozen ground has two regimes, namely transient followed by steady state. The transient flow regime is normally short compared with the steady state regime and is therefore not accounted for in their frozen ground infiltration model. The resulting correlation function is designed so that infiltration into frozen ground could be modelled in operational hydrology (Zhao and Gray 1999):

$$[8] \qquad \mathrm{INF} = CS_0^{2.92}(1 - S_\mathrm{I})^{1.64}[(273.15 - T_\mathrm{I})/273.15]^{-0.45}t^{0.44}$$

where INF is the cumulative infiltration (mm), C is the bulk coefficient that characterizes the effects on infiltration due to

© 2007 NRC Canada

differences between model and natural systems, S_I is the initial soil saturation (decimal), S_0 is the surface saturation (decimal), T_I is the initial soil temperature (°C), and t is the infiltration opportunity time (h). Through field testing, Zhao and Gray (1999) determined that the bulk coefficient $C = 1.3$ for boreal forests.

The frozen ground routine was initially tested for the 1991 and 1996 periods for the Taylor River watershed only, and the 1996 hydrographs are shown in Fig. 6. The frozen ground creates a significant amount of overland runoff, resulting in a steep hydrograph rising limb, a discharge peak with a short duration, and an equally steep receding limb. The fraction of the basin that contains frozen ground was lowered from 100% to 75%, 50%, 25%, and 10%. Correspondingly, the magnitude of runoff generation decreases as the fraction decreases. The first peak occurs on 19 May. The maximum infiltration rate varies between 6.6 and 11.4 mm/d over this period and results in approximately 10 mm of overland runoff when frozen soil is simulated for the entire basin. If the fraction of the basin with frozen ground is reduced to 25%, the overland flow decreases to 2.5 mm. The overland flow exits the basin quickly, resulting in a peak with a very short duration and a steep rising and receding limb. The observed hydrograph, however, is characterized by a steep rising limb but a slower receding limb. The frozen soil model does not account for the process responsible for this hydrograph characteristic. The year 1991 exhibits similar results. The bulk coefficient $C = 1.3$ results in low infiltration capacities on the order of 3.6–17.8 mm/d. The infiltration capacity increases to between 7.2 and 82.3 mm/d for the bulk coefficient $C = 6$. Additionally, the infiltration capacity is reduced quickly during the snowmelt period as the fast storage tank approaches capacity.

The second peak occurs on 1 June for the year 1996. The result is 20 mm of overland runoff between 29 May and 6 June. The total overland runoff is reduced to 7 mm if the fraction of the basin that is frozen is reduced to 25%. The receding limb is much steeper than the observed receding limb. Once the overland runoff exits the basin and the snowpack depletes entirely on 6 June, the total streamflow reduces to below the observed discharge, indicating that too little snowmelt and runoff are allocated to the soil storage zones. The simulation of the 19 May and 1 June discharge peaks is complicated by significant rain-on-snow events that likely modified the thermal characteristics of the snowmelt. The analysis carried out for 1991 does not have any significant rain-on-snow events during the majority of the snowmelt period; however, the results for 1991 are similar to those for 1996.

The inclusion of frozen ground causes significant overland runoff, which is the result of a combination of snowmelt and rainfall for 1991 and 1996. The runoff is of short duration and recedes too quickly, resulting in a significant underestimation in streamflow once the snowpack is depleted. The effects are mitigated but still present as the fraction of the basin containing frozen ground is reduced. The frozen ground routine developed by Zhao and Gray (1999) does not improve the SLURP hydrograph simulation during the snowmelt period because frozen ground does not likely generate significant amounts of excess runoff during the 1991 and 1996 periods.

Fig. 6. Simulated hydrographs for Taylor River for 1996 resulting from SLURP modified to include frozen soil with a bulk coefficient of $C = 1.3$.

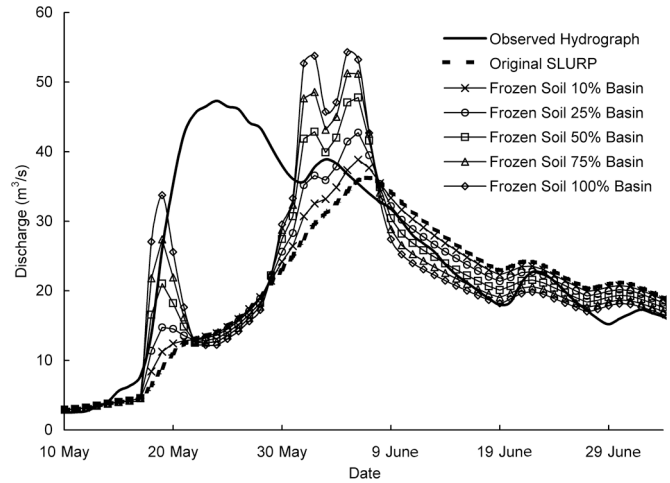

Snow processes

The majority of the observed hydrographs for both the Taylor River and upper Burntwood River share three common characteristics: the portion of the hydrograph prior to the spring freshet is very flat and shows little or no response to those days when temperatures exceed the melting point of snow; the rising limb during the spring freshet is very steep; and the peak flow during the spring freshet often but not always occurs shortly after the onset of snowmelt runoff. The SLURP model, on the other hand, exhibits premature generation of snowmelt, with some hydrographs showing response to those days when the temperature exceeds the melting point of snow. The simulated rising limb is not as steep as the observed rising limb, and the time of rise for the simulated hydrographs is commonly longer than the time of rise for the observed hydrographs. These deficiencies are likely caused by a few snowmelt processes that are not simulated by the SLURP model.

The snowpack undergoes a constant metamorphosis from the time that fresh snowfall is added to a snowpack until it is entirely converted to snowmelt. Freshly fallen snow is crystalline in structure, with sharply defined edges, and has a density of roughly 10% of liquid water. Over a period of hours, days, or weeks, the individual snow crystals become rounded and form large ice crystals, resulting in densities that can reach upwards of 50% of liquid water. In turn, the albedo of the snowpack decreases (ASCE 1996). The ambient temperature eventually raises the temperature of the top layer of the snowpack to 0 °C, causing some of the snow to be converted to water. Where the snowpack is 0 °C, there exists three forms of liquid water: (*i*) hygroscopic, or a thin film of water on the snow crystals; (*ii*) capillary, or water held by the surface tension of water; and (*iii*) gravitational, or water that moves downwards due to the force of gravity (Eagleson 1970). The gravitational water that moves downwards through the snowpack loses its heat energy to the lower parts of the snowpack, in turn causing the meltwater to refreeze and the temperature of the lower portion of the snowpack to rise. In time, the pack becomes isothermal at

© 2007 NRC Canada

0 °C and reaches a point in time where it contains significant hygroscopic and capillary water and no gravitational water. At this point the pack is said to be fully ripe. Any energy added to the fully ripe snowpack results in the production of gravitational water that exits the snowpack. This entire process is known as "snow ripening," which causes a delay in the production of meltwater that exits the snowpack.

Snow ripening

The degree-day approach for snowmelt modelling included in the SLURP model does not account for snow ripening. The method automatically generates snowmelt that exits the snowpack on any day when the average temperature exceeds the critical temperature. If the snow ripening process is included in the SLURP simulation, the start of the snowmelt runoff would be delayed, resulting in a greater release of snowmelt over a shorter period of time. This would result in an improved timing of snowmelt generation and a rising limb and peak that would resemble the observed hydrograph.

The use of a full energy budget is not a practical method for the SLURP model because many of the required inputs are not readily available. Methods for simulating snowpack ripening that use limited inputs have been available for many years and have not undergone many changes (Eagleson 1970; ASCE 1996; Melloh 1999). One of the most common inputs is the average daily air temperature. The air temperature can be assumed to equal the temperature near the surface of the snowpack. When the air temperature is averaged over a few days to allow for the penetration time constant of the thermal transients, this air temperature provides a satisfactory index of the portion of the heat deficit that is due to the capacity of the pack for sensible heat. This capacity is often called the cold content, W_c, of the snowpack and is defined as "the heat required per unit area to raise the temperature of the snowpack to 0 °C" (Eagleson 1970). The cold content is normally expressed "in terms of the amount of water needed to be produced at the surface to release energy by freezing" (ASCE 1996). This can be calculated by

$$[9] \qquad W_c = 0.5\rho_s d T_s'/80$$

where W_c is the cold content of the snowpack (mm), ρ_s is the average density of the snowpack (g/cm^3), d is the depth of the snowpack (mm), 0.5 is the specific heat of ice (cal/(g·°C), where 1 cal = 4.1868 J), T_s' is the average temperature deficit of the snowpack below 0 °C, and 80 is the latent heat of fusion of water (cal/cm^3). The computation of the cold content relies entirely on the temperature of the snowpack. In the case of a thin snowpack, the temperature of the snowpack can be assumed to equal the air temperature for the 1–3 d prior to the forecast time (ASCE 1996). This study uses a 3 d period prior to forecast time.

The snowpack is treated as an energy reservoir where snowmelt runoff is generated once the reservoir is full. This state coincides with the snowpack isothermal temperature of 0 °C. The cumulative temperature of the snowpack is determined with an index relation (ASCE 1996):

$$[10] \qquad T_s(2) = T_s(1) + F_p[T_a(2) - T_s(1)]$$

where T_s is the index of the snowpack surface temperature at times 1 and 2 (°C), T_a is the average air temperature of the 3 d period prior to the forecast time (°C), and F_p is a factor that varies between 0 and 1 and represents the relative penetration of the air temperature into the snowpack. A value of 0 indicates little penetration of the air temperature into the snowpack, causing a slow warming or cooling of the snowpack relative to the surrounding air temperature. The cold content of the snowpack is calculated using the following equation:

$$[11] \qquad W_c(2) = W_c(1) + C_r[T_a(2) - T_s(1)]$$

where W_c is the cold content at times 1 and 2 (mm), and C_r is the conversion factor (mm/(d·°C^{-1}). C_r functions identically to the snowmelt rate used in the snowmelt degree-day method and was set to that rate for this study. The snowpack becomes fully ripe once W_c reaches zero, thus permitting snowmelt to exit the snowpack.

Snowmelt rates

The literature recommends snowmelt rates between 1 and 5 mm/(d·°C^{-1}) for various types of land cover, but it was found that a January snowmelt rate of 0 mm/(d·°C^{-1}) and a July snowmelt rate of 0.5 mm/(d·°C^{-1}) provided optimum results in the original SLURP simulations. These two snowmelt rates minimized the magnitude of premature snowmelt runoff and best simulated the timing of the rising limb. The drawback of using the low snowmelt rates is a stunted hydrograph due to a prolonged snowmelt period. The implementation of a snow ripening routine controls the timing of initial snowmelt runoff generation. This eliminates a major modelling constraint when specifying the snowmelt rates, thus allowing the use of higher and more realistic snowmelt rates. The January and July snowmelt rates that were used in the original SLURP model were replaced by a single snowmelt rate R for the entire year. This removes the date dependency of the original snowmelt rates and eliminates one parameter from the model.

Application of the modified SLURP model

The modified SLURP model accommodates the larger snowmelt rates that are recommended in the literature because the snow ripening routine prevents premature snowmelt runoff. The modified SLURP was applied to the Taylor River watershed for the entire 16 year period. With the original parameters remaining unchanged, the snowmelt rates R for each land cover type were calibrated and the optimal values were found to be approximately 30% higher than the snowmelt rates determined by Metcalfe and Buttle (2001). The optimal snowmelt rates for the modified SLURP simulations were found to be 1.3 mm/(d·°C^{-1}) for coniferous and muskeg, 2.2 mm/(d·°C^{-1}) for deciduous and mixed, 3.8 mm/(d·°C^{-1}) for impervious, and 6.0 mm/(d·°C^{-1}) for water and marsh. In addition, F_p was calibrated for the Taylor River watershed, and the optimal value was found to be 0.10 for the entire simulation period.

The modified SLURP improved modelling results during the spring freshet period. Every year shows some improvement in the simulated hydrographs. The timing of initial snowmelt, that point where the cold content of the snowpack is satisfied and snowpack becomes ripe, is improved in

© 2007 NRC Canada

nearly all years. This results in a rising limb that occurs over a similar period compared with the observed hydrographs. This characteristic combined with the shorter and more intense snowmelt period results in a spring freshet with an improved time to peak and increased peak for most years. Many of the test years benefit from the higher peak discharge, with the exception of years such as 1987 and 1995. Figure 7 shows the observed and simulated hydrographs for 1986, both original and modified.

Figure 8 illustrates the snowpack depletion curves developed by the original and modified SLURP models for 1996. The curves demonstrate that snowpack depletes over a shorter period of time in the modified SLURP model. This causes the snowmelt to translate into runoff over a shorter period of time, resulting in a steeper rising limb. The slope of the rising limb in the simulation hydrographs improved and showed greater similarity to the observed hydrographs. The snowpack depletion curves also demonstrate that the snowpack is larger in the modified SLURP model relative to the original model. This occurs because less snowmelt is generated during the fall months. Even if temperatures sometimes rise above 0 °C, freshly fallen snow will partially ripen and refreeze. The original SLURP model does not account for this process and generates snowmelt in the fall months on any day when temperatures exceed the critical temperature.

Modelling efficiencies for the original and modified SLURP application on the Taylor River watershed were computed from the January–December, April–May, April, and May periods. The SLURP modification mainly impacted the spring freshet period, and therefore an evaluation of the statistics over the shorter periods amplifies any changes in the model results. With the exception of 3 years (1987, 1995, and 1998), the annual NSE improved significantly, an average of 6.5%. The April–May NSE also improved an average of 21.4%. The statistics for May exhibit the same trend, with an average increase in NSE of 39%. The April simulations showed the most improvement in NSE, but most values still remain below zero. The streamflow is normally very low during April, hence small errors in discharge relative to the mean April discharge result in a significant change in the NSE. The average annual DV increased by 0.7% for the 16 year period. This occurs as the volume of discharge increases during the spring freshet and does not cancel out as much of the excess discharge during the summer and fall months. The average DV for April–May, April, and May increased by 3.8%, 123%, and 2.4%, respectively.

In summary, simulations for April showed the greatest improvement due to the incorporation of snow ripening, delaying snowmelt generation. May also showed improvements in NSE and DV for most years because of the increased snowmelt intensity and greater snowpack available for snowmelt, resulting in a steeper rising limb and a higher spring freshet peak. Also, the snowmelt rates and melting characteristics are similar to those determined through field studies. For instance, open areas such as impervious and marsh areas are free of snow long before forested areas (Buttle et al. 2000).

For application to the upper Burntwood River watershed, F_p was the only value modified and it was increased from 0.100 to 0.125, which causes the snowpack to ripen faster and melt earlier. The modified SLURP improved the modelling results during the spring freshet period in a fashion similar to that for the Taylor River basin. The snow ripening routines delayed snowmelt and resulted in a delayed hydrograph response in all 16 test years. Most hydrographs improved with the delayed generation of snowmelt. Figure 9

Fig. 7. Simulated and observed hydrographs for Taylor River for 1986 from SLURP and modified SLURP. Dates are given as day/month/year.

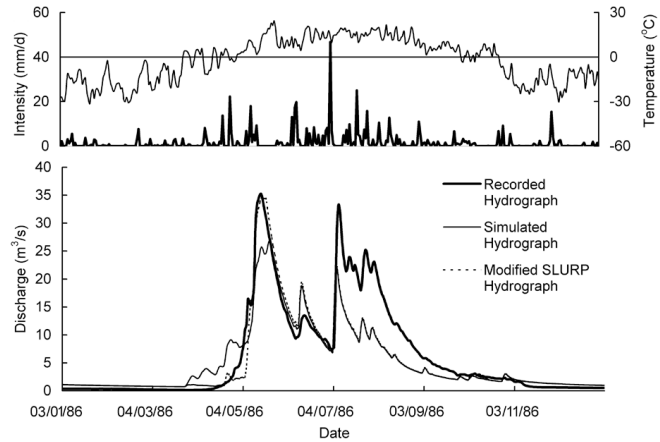

Fig. 8. Snowpack depletion curves for Taylor River for 1996 developed by (*a*) SLURP and (*b*) modified SLURP models.

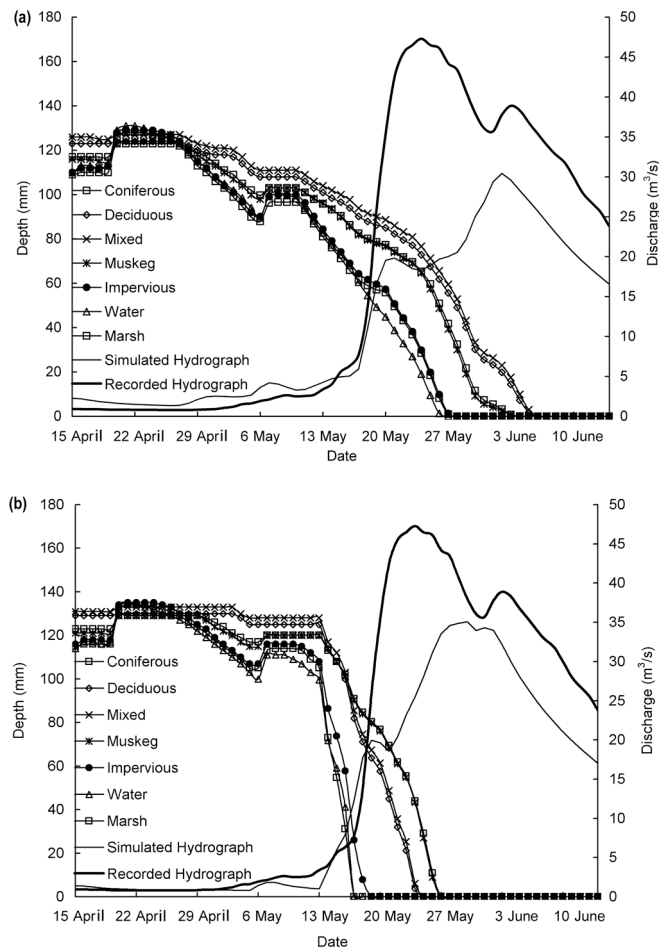

© 2007 NRC Canada

Fig. 9. Simulated and observed hydrographs for upper Burntwood River for 1992 from SLURP and modified SLURP. Dates are given as day/month/year.

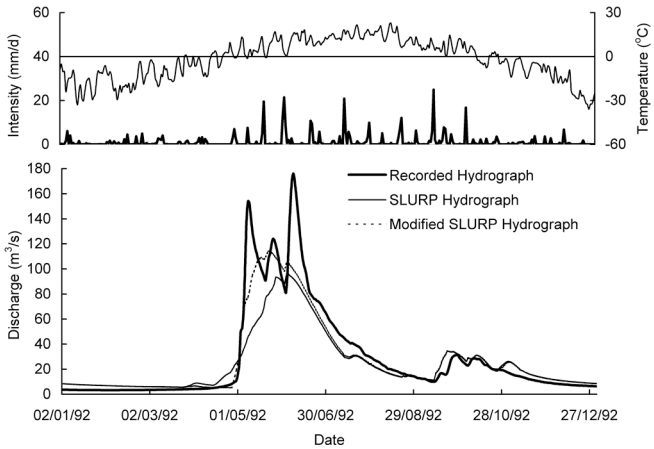

shows the observed and simulated hydrographs for 1992, both original and modified.

Modelling efficiencies for the original and modified SLURP application were also computed for the upper Burntwood River. Overall, the annual NSE decreased by 11.3% for each of the 16 test years. Nine of 16 years did not improve, with an average change in annual NSE of –26.6%. The remaining 7 years improved, with an average change in annual NSE of 8.3%. The average April–May NSE improved by 68.6%, but the average still remains below zero at –49.6%. The April NSE showed a significant improvement of 3494.1% but still remains below zero at –1914.2%. The average May NSE did not improve, although nearly half of the test years showed some improvement. A few years such as 1987, 1988, 1997, and 1998 showed a significant decrease in May NSE. The average annual DV decreased by –3.8% for the 16 year test period. The average April–May and May DVs also decreased by –0.8% and –7.5%, respectively. The average April DV showed a significant improvement of 53.5%, from ±123.7% to ±70.2%. It should be noted, however, that the April DV of ±70.2% is still far worse than the annual, April–May, and May DVs of ±25.2%, ±39.3%, and ±40.3%, respectively.

In summary, simulations for April again showed the most improvements. May also showed improvements in many years because of the increased snowmelt intensity and greater snowpack available for snowmelt, resulting in a steeper rising limb and a higher spring discharge peak. The results for the upper Burntwood River are considered satisfactory, considering the general quality and scarcity of meteorological input data, the diversity and quantity of the test years, and the use of nearly all the same parameters as those used for the Taylor River simulation.

Discussion

Based on this modelling effort, several findings and observations of the SLURP model were noted. The spring freshet normally produces the peak annual discharge and the majority of the annual streamflow and should therefore be the focus of modelling efforts. Most small and moderate rain events during the summer and fall months do not generate any runoff as a result of canopy and moss interception, depression storage, and subsequent evaporation. Only the largest rain events or a series of moderate rain events generate runoff. During significant rain events, the summer hydrographs are characterized by a steep rising limb and a longer receding limb but are short compared with the spring freshet. This indicates that the region has a flashy runoff response and a relatively small soil storage capacity. The differences in subsurface storage and interflow characteristics among the land covers are reflected in the subsurface model parameters. The forested covers have smaller upper soil storage capacity but higher retention constants relative to the muskeg cover, which is unable to hold water within the highly porous peat at high water levels.

The model was executed as one simulation from September 1984 to December 2000, and no backward correction of model state variables was applied during the simulation. It should be noted, however, that the 16 year test period used in this research is a relatively dry period, and future efforts could be directed to testing the model for other years that are significantly wetter. What is significant about this modelling effort and the implication to modelling in ungauged basins in this area is that a single parameter set was used to model important processes for both basins for a large number of test years containing diverse meteorological conditions that range from dry to moderately wet. The parameters are derived through both the literature and calibration, land cover specific, considered to be reasonable, and physically realistic. This is a considerable achievement given the constraints imposed on the modelling effort, including the following: (*i*) the scarcity of precipitation gauges and the significant variation in precipitation between the gauges; (*ii*) a single streamflow gauge was used for each basin during the model calibration and validation process; and (*iii*) the complex hydrologic processes that exist in the region of interest, some of which are not accounted for in the model. The parameters that did require site-specific calibration were the evapotranspiration-related parameters, which are often critical to calibration and accurate hydrograph generation. These parameters do differ between watersheds and are 23% higher in the upper Burntwood River watershed, but this is likely explained by the greater evaporation from lakes and depressions.

A number of modelling deficiencies were identified while learning about the study area and through model application. First, this research revised the model to account for a few hydrologic processes that resulted in improved modelling performance during the snowmelt period. Further to this, however, the model should be revised to include depression storage, its periodic disconnection with the drainage basin, and its associated evaporation losses. Second, the model would benefit by accounting for the recharge of water to lakes, rivers, and marshes by headwaters and the associated evaporation. The majority of marshes and beaver-flooded land are adjacent to lakes and rivers. A marsh to river linkage and a marsh to lake linkage that simulate the exchange of water between those bodies and the associated evaporation would improve modelling performance and the physical basis of the model. Third, since muskeg is a dominant land cover in the high boreal forest, attempts should be made to

© 2007 NRC Canada

improve the understanding of muskeg hydrology and better model the unique hydrology of this cover. For example, the exponentially decreasing hydraulic conductivity of muskeg results in a nonlinear retention of soil water and unique interflow characteristics. Lastly, ET models are very important in water yield estimates because they determine total basin losses. The various ET methods in the SLURP model should be tested and compared to each other and compared with field measurements such as those collected during the BOREAS field studies to test for accuracy. This exercise may determine that the SLURP model requires alternative ET models for the region of interest.

Further understanding of the hydrological processes in this watershed, and therefore the further development of models like SLURP, would greatly benefit from intensive monitoring programs that include the following: (*i*) year-round measurements of precipitation within the basins; (*ii*) streamflow gauges strategically located throughout the basin, including in the headwaters; (*iii*) measurements of snow depth, density, and cover; (*iv*) groundwater depth measurements in muskeg and coniferous forests to assist in characterizing soil moisture and aid in developing a better model for the muskeg cover; (*v*) water level measurements in marshes and lakes to assist in characterizing changes in storage and evaporation losses; and (*vi*) measurements of organic layer thickness, silty clay layer thickness, depth to bedrock, soil porosity, and hydraulic conductivity to assist in defining model soil characteristics.

Conclusions

The approaches employed in this study to modify a large-scale hydrological model for application to streamflow prediction for reservoir operations in the high northern boreal forest are relatively simple, yet these few and simple changes led to significant changes in modelling performance. This study therefore provides clues to the key processes that must be modelled in similar applications. Incorporating the snow ripening model delayed the snowmelt in nearly all years and prevented the premature generation of snowmelt that was created by the original SLURP model. Additionally, the snow ripening that occurred during the fall months is also accounted for and results in less snowmelt in the fall and a larger snowpack in the following spring. The larger snowmelt rates recommended in the literature could be used in the modified SLURP model and were increased by 30% to provide optimum snowmelt characteristics. The higher snowmelt rates caused a faster snowmelt, resulting in a shorter snowmelt period, less sublimation, and more total snowmelt runoff volume. The slope of the hydrograph rising limb, time to peak, and magnitude of the peak improved in most years.

Acknowledgements

The authors would like to thank Manitoba Hydro and the Natural Sciences and Engineering Research Council of Canada (NSERC) for funding this work. The authors would also like to thank C.L.I. Ho, B. Girling, E. Teklemariam, B. Korbaylo, C.M. Fast, D.U.H. Tang, and Linnet Geomatics for all their assistance. Lastly, thanks to the reviewers for their insightful comments.

References

Agriculture Canada. 1986. Soil landscapes of Canada — Manitoba. Publication 5242/B, Land Resource Research Centre, Research Branch, Agriculture Canada, Ottawa, Ont.

Anderson, E.A., and Neuman, P.J. 1984. Inclusion of frozen ground effects in a flood forecasting model. *In* Proceedings of the 5th Northern Research Basin Symposium: The Role of Snow and Ice in Northern Basin Hydrology, Vierumaki, Finland, 19–23 March 1984. pp. 5.1–5.14.

ASCE. 1996. Hydrology handbook. 2nd ed. ASCE Manuals and Reports on Engineering Practice No. 28, American Society of Civil Engineers (ASCE), New York.

Beven, K.J. 2000. Rainfall–runoff modelling: the primer. John Wiley & Sons, Chichester, UK.

Biftu, G.F., and Gan, T.Y. 2001. Semi-distributed, physically-based, hydrologic modeling of the Paddle River Basin, in Alberta, using remotely-sensed data. Journal of Hydrology, **244**: 137–156.

Bingeman, A.K., Kouwen, N., and Soulis, E.D. 2006. Validation of the hydrological processes in a hydrological model. Journal of Hydrologic Engineering, **11**(5): 451–463.

Brown, R.J.E. 1977. Forests, muskeg, and organic terrain. *In* Muskeg and the northern environment in Canada. *Edited by* N.W. Radforth and C.O. Brawner. University of Toronto Press, Toronto, Ont. pp. 148–163.

Buttle, J.M., Creed, I.F., and Pomeroy, J.W. 2000. Advances in Canadian forest hydrology, 1995–1998. Hydrological Processes, **14**: 1551–1578.

Chen, J.M., Chen, X., Ju, W., and Geng, X. 2005. Distributed hydrological model for mapping evapotranspiration using remote sensing inputs. Journal of Hydrology, **305**: 15–39.

Crippen Acres Wardrop. 1990. Nelson River flood study: Phase II. Report prepared for Generation Planning Division, Manitoba Hydro, Winnipeg, Man.

Eagleson, P.S. 1970. Dynamic hydrology. McGraw-Hill Book Company, New York.

Goode, D.A., Marsan, A.A., and Michaud, J.R. 1977. Water resources. *In* Muskeg and the northern environment in Canada. *Edited by* N.W. Radforth and C.O. Brawner. University of Toronto Press, Toronto, Ont. pp. 299–331.

Grelle, A., Lundberg, A., Lindroth, A., Morén, S., and Cienciala, E. 1997. Evaporation components of a boreal forest: variations during the growing season. Journal of Hydrology, **197**: 70–87.

Haberlandt, U., and Kite, G.W. 1998. Estimation of daily space–time precipitation series for macroscale hydrological modelling. Hydrological Processes, **12**(9): 1419–1432.

Kite, G.W. 1978. Development of a hydrologic model for a Canadian watershed. Canadian Journal of Civil Engineering, **5**: 126–134.

Kite, G.W. 1991. A watershed model using satellite data applied to a mountain basin in Canada. Journal of Hydrology, **128**: 157–169.

Kite, G.W. 1995. Use of remotely sensed data in the hydrological modeling of the upper Columbia watershed. Canadian Journal of Remote Sensing, **22**(1): 14–22.

Kite, G.W. 1997. Manual for the SLURP hydrological model V.11. National Hydrology Research Institute, Saskatoon, Sask.

Kite, G.W. 1998. Simulating long series of streamflow using data from an atmospheric model. Hydrological Sciences, **43**(3): 391–407.

Kite, G.W. 2002. Manual for the Slurp hydrological model 12.2. Hydrologic Solutions, Abingdon, Oxfordshire, UK.

Kite, G.W., and Spence, C.D. 1994. Land cover, NDVI, LAI, and evapotranspiration in hydrological modelling. *In* Applications of Remote Sensing in Hydrology: Proceedings of the 2nd Interna-

© 2007 NRC Canada

tional Workshop, Saskatoon, Sask., 18–20 October 1994. *Edited by* G.W. Kite, A. Pietroniro, and T.J. Pultz. NHRI Symposium 14, National Hydrology Research Institute (NHRI), Saskatoon, Sask. pp. 223–240.

Kite, G.W., Dalton, A., and Dion, K. 1994. Simulation of streamflow in a macroscale watershed using general circulation model data. Water Resources Research, **30**(5): 1547–1559.

Leese, J.A. 1993. Implementation plan for the GEWEX continental-scale international project (GCIP). Vol. I. Data collection and operational model upgrade. Publication Series 6, World Climate Research Program, International GEWEX Project Office (IGO), Silver Spring, Md.

McKnight, T.L. 1993. Physical geography: a landscape appreciation. Prentice Hall Inc., Englewood Cliffs, N.J.

Melloh, R.A. 1999. A synopsis and comparison of selected snowmelt algorithms. CRREL Report 99-8, Cold Regions Research and Engineering Laboratory (CRREL), Hanover, N.H.

Metcalfe, R.A., and Buttle, J.M. 1999. Semi-distributed water balance dynamics in a small boreal forest basin. Journal of Hydrology, **226**: 66–87.

Metcalfe, R.A., and Buttle, J.M. 2001. Soil partitioning and surface store controls on spring runoff from a boreal forest peatland basin in north-central Manitoba, Canada. Hydrological Processes, **15**: 2305–2324.

Nash, J.E., and Sutcliffe, J.V. 1970. River flow forecasting through conceptual codels: part 1 — a discussion of principles. Journal of Hydrology, **10**(3): 282–290.

Newcomer, J., Landis, D., Conrad, S., Curd, S., Huemmrich, K., Knapp, D., Morrell, A., Nickeson, J., Papagno, A., Rinker, D., Strub, R., Twine, T., Hall, F., and Sellers, P. (*Editors*). 2000. Collected data of the boreal ecosystem–atmosphere study [online]. National Aeronautics and Space Administration (NASA), Oak Ridge, Tenn. Available from http://www.daac.ornl.gov [accessed 30 September 2001].

Nickeson, J., Landis, D., and Hall, F.G. (*Editors*). 2002. Collected data of the boreal ecosystem–atmosphere study follow-on [online]. National Aeronautics and Space Administration (NASA), Oak Ridge, Tenn. Available from http://www.daac.ornl.gov [accessed 30 September 2001].

Nyberg, L., Manfred, S., Mellander, P., and Bishop, K.H. 2001. Soil frost effects on soil water and runoff dynamics along a boreal forest transect: 1. Field investigations. Hydrological Processes, **15**: 909–926.

Peddle, D.R., and Franklin, S.E. 1993. Classification of permafrost active layer depth from remotely sensed and topographic evidence. Remote Sensing of Environment, **40**: 67–80.

Phersson, M., and Pettersson, O. 1997. Energy and water balance of a bog in central Sweden. Nordic Hydrology, **28**(4/5): 263–272.

Price, A.G., Dunham, K., Carleton, T., and Band, L. 1997. Variability of water fluxes through the black spruce (*Picea mariana*) canopy and feather moss (*Pleurozium schreberi*) carpet in the boreal forest of northern Manitoba. Journal of Hydrology, **196**: 310–323.

Radforth, N.W., and Brawner, C.O. (*Editors*). 1977. Muskeg and the northern environment in Canada. University of Toronto Press, Toronto, Ont.

Saxton, K.E. 2002. Soil water characteristics — hydraulic properties calculator [online]. Biological Systems Engineering, Washington State University, Pullman, Wash. Available from http://www.bsyse.wsu.edu/saxton/soilwater/ [accessed 15 April 2002].

Sellers, P., Hall, F.G., Kelly, R.D., Black, A., Baldocchi, D., Berry, J., Ryan, M., Ranson, K.J., Crill, P.M., Lettenmaier, D.P., Margolis, H., Cihlar, J., Newcomer, J., Fitzjarrald, D., Jarvis, P.G., Gower, S.T., Halliwell, D., Williams, D., Goodison, B., Wickland, D.E., and Guertin, F.E. 1997. BOREAS in 1997: experiment overview, scientific results, and future directions. Journal of Geophysical Research, **102**(D24): 28 731 – 28 769.

Spittlehouse, D.L. 1989. Estimating evapotranspiration from land surfaces in British Columbia. *In* Estimation of areal evapotranspiration. *Edited by* T.A. Black, D.L. Spittlehouse, M.D. Novak, and D.T. Price. IAHS Publication 177, IAHS Press, Wallingford, UK. pp. 245–253.

Stolte, W.J., and Van der Kamp, G. 1999. Modelling wetland hydrology using modified SLURP. *In* Proceedings of the 14th Hydrotechnical Specialty Conference of the Canadian Society for Civil Engineering, Regina, Sask., 2–5 June 1999. *Edited by* R.S. Pentland. Canadian Society for Civil Engineering, Montréal, Que. Vol. 2, pp. 405–415.

Yin, Z., and Williams, T.H.L. 1997. Obtaining spatial and temporal vegetation data from Landsat MSS and AVHRR/NOAA satellite images for a hydrologic model. Photogrammetric Engineering & Remote Sensing, **63**(1): 69–77.

Zhao, L., and Gray, D.M. 1997. A parametric expression for estimating infiltration into frozen soils. Hydrological Processes, **11**: 1761–1775.

Zhao, L., and Gray, D.M. 1999. Estimating snowmelt infiltration into frozen soils. Hydrological Processes, **13**: 1827–1842.

© 2007 NRC Canada

Copyright of Canadian Journal of Civil Engineering is the property of NRC Research Press and its content may not be copied or emailed to multiple sites or posted to a listserv without the copyright holder's express written permission. However, users may print, download, or email articles for individual use.